frontiers | Frontiers in Marine Science

TYPE Original Research
PUBLISHED 02 September 2022
DOI 10.3389/fmars.2022.989454

OPEN ACCESS

EDITED BY
Yunyan Deng,
Institute of Oceanology, (CAS), China

REVIEWED BY
Jin-Yan Zhang,
Yunnan Agricultural University, China
Shailendra Pratap Singh,
Institute of Science, Banaras Hindu University, India
Paul M. D'Agostino,
Technical University Dresden, Germany

*CORRESPONDENCE
Ulf Karsten
ulf.karsten@uni-rostock.de

SPECIALTY SECTION
This article was submitted to Marine Biology, a section of the journal Frontiers in Marine Science

RECEIVED 08 July 2022
ACCEPTED 15 August 2022
PUBLISHED 02 September 2022

CITATION
Borburema HDS, Graiff A, Marinho-Soriano E and Karsten U (2022) Photosynthetic performance, growth, pigment content, and photoprotective compounds of the mangrove macroalgae *Bostrychia calliptera* and *Bostrychia montagnei* (Rhodophyta) under light stress.
Front. Mar. Sci. 9:989454.
doi: 10.3389/fmars.2022.989454

Photosynthetic performance, growth, pigment content, and photoprotective compounds of the mangrove macroalgae *Bostrychia calliptera* and *Bostrychia montagnei* (Rhodophyta) under light stress

Henrique D. S. Borburema[1], Angelika Graiff[2], Eliane Marinho-Soriano[1] and Ulf Karsten[2]*

[1]Department of Oceanography and Limnology, Biosciences Institute, Federal University of Rio Grande do Norte, Natal, Brazil, [2]Institute of Biological Sciences, Applied Ecology and Phycology, University of Rostock, Rostock, Germany

Increased solar radiation on the Earth's surface is expected due to global change. Mangrove macroalgae can be negatively affected by increased solar radiation, since some species, such as *Bostrychia* spp. have been characterized as typical "shade" plants. Thus, we investigated the effects of increasing photon flux densities (PFDs: 170, 267, 443, 638, and 1155 µmol photons m^{-2} s^{-1}) on the physiological performance of *Bostrychia calliptera* and *Bostrychia montagnei* from a tropical mangrove. Several photosynthesis–related parameters indicated that both species decreased their photosynthetic performance under increasing PFDs, with photosynthesis of *B. montagnei* being more affected than that of *B. calliptera*. *Bostrychia calliptera* exhibited highest growth under 638 µmol photons m^{-2} s^{-1} while at 1155 µmol photons m^{-2} s^{-1} it was inhibited. The highest growth of *Bostrychia montagnei* was observed under 267 µmol photons m^{-2} s^{-1}. Higher PFDs led to growth inhibition. The phycobiliprotein and chlorophyll *a* content of *B. montagnei* was degraded under increased PFDs. In *B. calliptera* only chlorophyll *a* degradation was observed. The mycosporine-like amino acid contents (photoprotective metabolites) of both species were degraded under increasing PFDs, which was more pronounced in *B. montagnei*. Our results demonstrated that increased solar radiation on estuarine tropical ecosystems will be detrimental to the physiological performance of *B. calliptera* and *B. montagnei*. Our results also demonstrated that *B. montagnei* was more negatively affected by increased light stress than *B. calliptera*. This can explain its preferential occurrence in more shaded microhabitats compared to *B. calliptera*. Our data document for the first time light acclimation in the studied macroalgae and the deleterious effects of increased light stress on the genus *Bostrychia*.

KEYWORDS

global change, increased solar radiation, macroalgal segregation, mycosporine-like amino acids (MAAs), pigment degradation

Introduction

Global change due to the increasing anthropogenic emissions of greenhouse gases into the Earth's atmosphere is an ecologically serious problem (IPCC, 2019). Fluorinated gases emitted into the atmosphere, such as chlorofluorocarbons, hydrofluorocarbons, and perfluorocarbons in addition to being greenhouse gases lead to stratospheric ozone depletion (IPCC, 2014). The stratospheric ozone forms a filtering layer against biologically harmful solar radiation on the Earth, mainly ultraviolet radiation A (320–400 nm) and B (280–320 nm) (Madronich, 1992; Karsten, 2008). Thus, an increase in harmful solar radiation on the Earth's surface is documented due to the depletion of the stratospheric ozone layer (Thomas et al., 2012). Enhanced solar radiation on coastal ecosystems can trigger several detrimental effects on photosynthetic organisms, for example, DNA alterations, biosynthesis of reactive oxygen species (ROS), photoinhibition, degradation of photosynthetic pigments, and changes in the ultrastructure of cells, such as, increased thickness of cell wall, reduced intracellular spaces, and destruction of chloroplast internal organization (Van de Poll et al., 2001; Schmidt et al., 2012; Kaur et al., 2022).

Although light commonly is a primary driver of increases in macroalgal coverage (Scherrer et al., 2019), excessive irradiance is an additional stress factor that phototrophic organisms have to cope with in their respective environments (Diehl et al., 2019). Macroalgal species that are sensitive to high irradiance preferentially inhabit shaded habitats, where they are protected from full sun exposure, and hence are characterized as typical "shade" plants (Raven et al., 1979; Coutinho and Yoneshigue, 1988). The red algal genus *Bostrychia* Montagne occurs preferentially in tropical and subtropical mangrove swamps and in temperate salt marshes (King and Puttock, 1989). In mangrove ecosystems, in the intertidal zones, *Bostrychia* species grow as epiphytes on rhizophores and trunks of *Rhizophora* L. and *Laguncularia* C. F. Gaertn, and on pneumatophores of *Avicennia* L. (West et al., 1992; Pedroche et al., 1995). Growing on these biogenic hard substrates they are protected from full sunlight exposure by the covering canopy (Karsten et al., 1994a; Karsten et al., 1996). *Bostrychia* species grow forming turfs on the mangrove trees along with other associated red macroalgae, such as *Caloglossa* (Harvey) G. Martens and *Catenella* Greville (King and Puttock, 1989). These macroalgae form an intertidal plant association termed Bostrychietum (Post, 1936). This algal association can also be considered an ecological strategy to decrease the light stress for individual algae, since they grow on top of each other and accumulate estuarine sediment particles on the surfaces of the branches. In addition to these ecological strategies, *Bostrychia* species synthesize and accumulate photoprotective secondary metabolites against ultraviolet radiation (Karsten et al., 1998; Lalegerie et al., 2019; Orfanoudaki et al., 2019; Karsten et al., 2000; Orfanoudaki et al., 2020; Gambichler et al., 2021a). These UV–absorbing compounds form a class of water-soluble metabolites of low molecular weight chemically assigned as mycosporine-like amino acids (MAAs) (Karsten, 2008). *Bostrychia* species can also occur in intertidal reefs and on rocky shores (King and Puttock, 1989; Machado et al., 2011), inhabiting crevices, cavities or other places protected from full solar radiation (Karsten and Kirst, 1989). Several studies have demonstrated that *Bostrychia* species are typical "shade" plants, because of the low light requirements for photosynthesis (e.g., Karsten and Kirst, 1989; Karsten et al., 1993; Karsten et al., 1994a; Karsten et al., 1994b; Sánchez de Pedro et al., 2014). However, studies reporting the effects of increasing light stress on *Bostrychia* species are still lacking in the scientific literature. Considering future environmental conditions of increased solar radiation on coastal ecosystems due to global change, such ecophysiological studies are needed.

In estuarine environments *Bostrychia* species perform relevant ecosystem services. Along with microalgae they are major sources of primary productivity (Karsten et al., 1994a; Karsten et al., 2000), contributing to the CO_2 sequestration in mangrove swamps (Kieckbusch et al., 2004; Borburema et al., 2022a). The Bostrychietum is an important microhabitat for several invertebrates (García et al., 2016; Vieira et al., 2018; Borburema et al., 2021), and some *Bostrychia* species are recognized as bioindicators of estuarine contamination by heavy metals (Melville and Pulkownik, 2006; Melville and Pulkownik, 2007; Rios-Marin et al., 2021). In Brazilian mangroves, among *Bostrychia* species, *Bostrychia calliptera* (Montagne) Montagne and *Bostrychia montagnei* Harvey occur with high predominance (Yokoya et al., 1999; Cunha and Costa, 2002; Fontes et al., 2007; Machado and Nassar, 2007; Mendonça and Lana, 2021).

Currently, *in vivo* chlorophyll *a* fluorescence measurements have been used to estimate the photosynthetic activity of macroalgae under stress conditions (Figueroa et al., 2014; Figueroa et al., 2019). Fluorescence measurements are of great interest for ecological studies, since they are based on a non-invasive method and suitable to track *in vivo* stress responses of macroalgae (Figueroa et al., 2019). Fluorescence techniques have been extensively used to estimate the photosynthetic performance of marine phototrophic organisms during the last 20 years (Figueroa et al., 2019). However, the photosynthetic performance of *Bostrychia* species was only recently estimated using fluorescence techniques after species had been subjected to salt stress (Gambichler et al., 2021b), desiccation stress (Sánchez de Pedro et al., 2022), ocean acidification (Borburema et al., 2022a), and to temperature and salinity stress (Borburema et al., 2022b). Photosynthetic performance of *Bostrychia* species based on chlorophyll *a* fluorescence after specimens have been subjected to light stress has not yet been explored.

In the present study, we investigated the effects of increasing photon flux densities on the physiological performance of the mangrove macroalgae *B. calliptera* and *B. montagnei* to address the following question: How can future environmental conditions of enhanced solar radiation on coastal ecosystems due to global change affect these macroalgal species? We hypothesized that: (i) increase in light will be detrimental to the physiological performance of the macroalgae, since they are typical "shade" plants; (ii) *B. calliptera* will be more tolerant to increasing light stress than *B. montagnei*, since *B. montagnei* occurs preferentially in more shaded microhabitats compared to *B. calliptera*, as documented by Yokoya et al. (1999); and (iii) both species will increase their MAA contents under increased light conditions.

Materials and methods

Algal collections and cultures

Thalli of *B. calliptera* and *B. montagnei* were collected in the mangrove swamp of Mamanguape River Estuary Environmental Protection Area (6°46'15.00"S and 34°56'15.00"W), Paraíba state, Brazil, in September 2021. Both red algae were collected from rhizophores of *Rhizophora mangle* L. during low tide. Algal collection was authorized by ICMBio/Brazil (authorization n° 65168–1), since it was carried out within Brazilian conservation unit. The algal collection site is located in Northeastern Brazil, a tropical semi-arid climate region where only two seasons occur, a dry season from September to February (spring/summer) and a rainy season from March to August (autumn/winter) (Sassi et al., 1988). Mean global solar radiation on the algal collection area over the dry season is higher and varies from 220 to 280 W m^{-2}, whereas over the rainy season it varies from 140 to 220 W m^{-2} (INPE, 2022). The photoperiod is around 12–13 h in both seasons and based on historical series (2013–2018), the mean photosynthetically active radiation (PAR) on the algal collection area is around 220 W m^{-2} (INPE, 2022), which corresponds to about 2935 µmol photons m^{-2} s^{-1} (Valiela, 1984). In general, in Northeastern Brazil, the ultraviolet radiation (UVR) reaches very high values (Ultraviolet Index from 8 to 10) during most of the year between 10:30 a.m. and 3:00 p.m. (INPE, 2022).

During the field collection, most of the estuarine sediment was removed from the thalli with estuary water. Afterward, the specimens were transported to the laboratory of marine macroalgae of Federal University of Rio Grande do Norte (Brazil) in thermally insulated boxes at a temperature of around 20°C and in darkness. In the laboratory, the remaining sediment adhered on the thalli was removed by several washing and spraying with UV–sterilized and filtered seawater. Thalli parts with filamentous macroalgae were removed by cutting with scalpels and macrofauna individuals were removed with tweezers, both under a stereomicroscope. After these procedures, the macroalgae were transported to the laboratory of Applied Ecology and Phycology of the University of Rostock (Germany) in thermally insulated bags at a temperature of around 20°C and in darkness, for the establishment of unialgal cultures and light stress experiments, as described below.

The macroalgae (biomass around 5 g L^{-1}) were washed with deionized water, gently blotted dry with paper towels, and maintained in continuous immersion in 1 L Erlenmeyer flasks containing 800 mL of culture medium. The culture medium consisted of natural seawater (adjusted absolute salinity of 30–32 S_A) sterilized by filtering enriched with Provasoli's solution (PES/2) (Starr and Zeikus, 1993). The culture medium was aerated continuously and replaced weekly for nutrient replenishment. Algae were maintained under a water temperature of 21–24°C, a photon flux density (PFD) of 160–190 µmol photons m^{-2} s^{-1} provided by cool-white fluorescent tubes (Osram L36W/840, Lumilux, Germany), and a light: dark cycle of 16: 8 h (Karsten et al., 1994a). Both red algae remained in these conditions for a nine–week acclimation period, after which they were experimentally cultured. Photon flux density was measured with a quantum photometer (LI–250, LI–COR, USA) attached to a spherical LI–COR quantum sensor (US–SQS/L, Walz, Germany).

Experimental design

Vegetative thalli of *B. calliptera* and *B. montagnei* were cultured for 14 days under increasing PFDs of 170, 267, 443, 638, and 1155 µmol photons m^{-2} s^{-1}. The mean PAR on the algal collection area is around 2935 µmol photons m^{-2} s^{-1}, as described in the previous section. After attenuation by the covering canopy the mean proportions of incident PAR on the Bostrychietum of Brazilian mangroves are around 5, 8, and 17% (Yokoya et al., 1999). These percentages of incident PAR were

calculated by Yokoya et al. (1999) as the ratio between PAR at ground level and above the canopy. They varied depending on the density of the covering canopy. The first three applied PFDs were established following the PAR proportions revealed by Yokoya et al. (1999), whereas the last two were established as increased PFD conditions due to global change. Each PFD was established in particular chambers of two temperature– and photoperiod–controlled incubators (one for each species). Each particular chamber was equipped with LED lights on top, which were adjusted to produce the target PFDs. For the experiment, the target PFDs were also measured using the quantum photometer attached to the spherical LI–COR quantum sensor. Thalli were cultured in 50 mL transparent culture flasks (Cellstar®, Greiner Bio–One, Germany) containing 40 mL of culture medium (as described above). The culture medium was replaced after seven days for nutrient replenishment. Ten treatments were established (two species × five PFDs) and each treatment had four independent replicates (n = 4). Each replicate consisted of two apical branches (2–3 cm in primary axis length) with laterals of the macroalgae. The initial biomass per replicate for *B. calliptera* and *B. montagnei* was of 57 ± 3 mg and 66 ± 5 mg, respectively. The macroalgae were cultured at a temperature of 25 ± 1 °C (Borburema et al., 2020) and under a light: dark cycle of 14: 10 h (Borburema et al., 2022a). The UV radiation of each treatment was measured using UVA and UVB sensors connected to a data logging radiometer (PMA2100, Solar light®, USA). The UVA was 0.01 W m^{-2} in all treatments and UVB was not detected.

Photosynthetic performance

In vivo chlorophyll *a* (Chl *a*) fluorescence measurements were obtained from one random branch of each replicate (n = 4) using a Pulse Amplitude Modulated (PAM) fluorometer (PAM–2500, Walz, Germany) to calculate several photosynthetic parameters of the macroalgae. Before culturing the red algae under different PFDs, and every seven days during the experiment, the effective quantum yield ($\Delta F/F_m'$) of photosystem II (PSII) was calculated. The formula $\Delta F/F_m' = (F_m' - F_t)/F_m'$ was used, where F_t is the current steady–state fluorescence of light–adapted algae and F_m' is the maximum fluorescence of the algae under actinic light during a saturating pulse (Schreiber et al., 1995). F_t was measured under a very low photon fluence rate of red light (0.05 µmol photons m^{-2} s^{-1}) and F_m' during a saturating pulse of 0.5 s.

On the last experimental day, after measuring F_t and F_m' to calculate $\Delta F/F_m'$, the branches were dark–acclimated for 15 min. Subsequently, light pulses (2, 6, 64, 101, 141, 198, 271, 363, 474, 619, and 785 µmol photons m^{-2} s^{-1}) were applied in 20 s intervals to construct relative electron transport rate (rETR) vs. photon fluence rate (PAR) curves. From the first light pulse the maximum quantum yield (F_v/F_m) of PSII was calculated using the formula $F_v/F_m = (F_m - F_o)/F_m$, where F_m is the maximum fluorescence during a saturating pulse on dark–acclimated algae and F_o is the basal fluorescence (Schreiber et al., 1995; Suggett et al., 2011). Relative electron transport rates were calculated by multiplying the $\Delta F/F_m'$ with the appropriate PAR values ($rETR = \Delta F/F_m' \times PAR$) (Schreiber et al., 1995; Suggett et al., 2011). Relative electron transport rate vs. photon fluence rate curves were fitted applying the mathematical model of Walsby (1997), due to the presence of photoinhibition. From each curve, the maximum relative electron transport rate ($rETR_{max}$), the light utilization coefficient (α), the photoinhibition coefficient (β), and the initial saturation irradiance for photosynthesis (I_k) were calculated.

For each light treatment, complementary energy dissipation pathways in PSII were investigated. The photochemical pathway was calculated as $Y(II) = (F_m' - F_t)/F_m'$, whereas the non-regulated non-photochemical quenching of light energy (Y [NO]) was determined using the formula $Y(NO) = F_t/F_m$, and the regulated non-photochemical quenching of light energy (Y [NPQ]) was calculated using the formula $Y(NPQ) = F_t/F_m' - Y(NO)$. The Y(NO) reflects the fraction of energy that is passively dissipated in form of heat and fluorescence, mainly due to closed PSII reaction centers, while Y(NPQ) corresponds to the fraction of energy dissipated in form of heat *via* the regulated photoprotective non-photochemical quenching mechanisms (Scherner et al., 2013). Overall, the total energy is conserved as Y(II) + Y(NPQ) + Y(NO) = 1.

Relative growth rates

At the end of the experiment, after measuring Chl *a* fluorescence, the branches were gently blotted dry with paper towels to remove excess water and weighed on an analytical balance to estimate their relative growth rates (RGRs). The RGRs were calculated using the equation recommended by Yong et al. (2013): $RGR=[(W_t/W_i)^{1/t}- 1]\times100$, where W_i and W_t are the initial and final wet weights, respectively, and t is the culture period.

Biochemical analyses

Algal biomass of each replicate (n = 4) was washed with deionized water to remove the salt on the branches, gently blotted dry with paper towels, weighed, and stored in microtubes for further biochemical analyses. The algal samples were frozen in liquid nitrogen and kept at -20°C and protected from light for further analyses of pigment contents and mycosporine–like amino acids, as described below.

Pigment content

For each replicate (n = 4), a biomass of 55 mg ± 1 of wet weight (WW) was powdered in liquid nitrogen using mortar and pestle. Phycobiliproteins – phycoerythrin (PE), phycocyanin

(PC), and allophycocyanin (APC) – were extracted in 1 mL of 50 mM sodium phosphate (Na_2HPO_4) buffer (pH 5.5) overnight at 4°C and protected from light (Souza and Yokoya, 2016). Afterward, the samples were centrifuged (Centrifuge 1–14K, Sigma, Germany) at 12,000×g for 20 min at 4°C. Absorbances in the supernatants were measured by spectrophotometry (Spectrophotometer UV–2401 PC, Shimadzu, λ = 498.5, 614, and 651 nm), and the phycobiliprotein concentrations in the alga (μg g^{-1} of WW) were determined using the equations proposed by Kursar et al. (1983):

$$PE = [(155.8 \times A_{498.5}) - (40 \times A_{614}) - (10.5 \times A_{651})] \times WW^{-1}$$

$$PC = [(151.1 \times A_{614}) - (99.1 \times A_{651})] \times WW^{-1}$$

$$APC = [(181.3 \times A_{651}) - (22.3 \times A_{614})] \times WW^{-1}$$

Pellets were resuspended in 1 mL of 90% acetone to extract Chl *a* for 1 h at 4 °C and protected from light (Borburema et al., 2022b). Afterward, the samples were centrifuged at 12,000×g for 15 min at 4 °C. Absorbances in the supernatants were measured by spectrophotometry (λ = 630, 647, and 664 nm), and the quantification of Chl *a* in the alga (μg g^{-1} of WW) was carried out following the equation below given by Jeffrey and Humphrey (1975). In addition, the absorbance spectrum of Chl extracts was measured by spectrophotometry (λ = 400–800 nm).

$$\text{Chl } a = [(11.85 \times A_{664}) - (1.54 \times A_{647}) - (0.08 \times A_{630})] \times WW^{-1}$$

Mycosporine-like amino acid content

Algal biomass of each replicate (n = 4) was used for mycosporine–like amino acid analyses by High Performance Liquid Chromatography (HPLC) (Karsten et al., 2000). Macroalgae were lyophilized in a freeze–drier (CDplus, Christ, Germany) and posteriorly powdered using mortar and pestle. Mycosporine–like amino acids (MAAs) were extracted from the powdered algal samples (10 mg of dry weight – DW) in 1 mL of aqueous 25% methanol (v/v, HPLC grade) in a water bath (45°C) for 4 hours. During the extraction time in the water bath, the samples were vortexed regularly (Vortex–Genie 2, Scientific Industries, USA) to optimize extraction. Afterward, the samples were centrifuged at 13,000×g for 15 min (Biofuge pico, Heraeus, Germany) and the methanolic supernatants were transferred to new microtubes, followed by evaporation to dryness in a Speed Vacuum Concentrator (RVC 2–25 CDplus, Christ, Germany). Afterward, the dried pellets were re-dissolved in 1 mL of HPLC water. Aqueous homogenates were vortexed for 30 s and then centrifuged at 13,000×g for 15 min. Finally, the aqueous supernatants were transferred to HPLC vials after passing through a 0.45 μm filter (WhatmanTM, Germany) prior injection onto the HPLC column.

Mycosporine–like amino acids in the samples were analyzed qualitatively and quantitatively using a 1220 Infinity II HPLC system (Agilent Technologies, Germany) with a diode array detector (DAD: 330 nm, range: 240–400 nm). A Phenomenex Synergie 4μ fusion RP column (C18, 4 μm, 250 × 3mm, Phenomenex, Germany) protected by a guard cartridge (RP-18 4 × 3 mm I.D., Phenomenex) was used to identify MAAs. During measurements the mobile phase (eluent) was 2.5% methanol (v/v) plus 0.1% acetic acid (v/v) with a flow rate of 0.5 mL min^{-1}, 150 bar pressure, column temperature at 30 °C, and 10 μL as the injection volume. The sample chromatograms (Figure S1) were compared with those from the biological standards of palythine, asterina–330, shinorine, and porphyra–334 to identify MAAs by retention time and absorbance spectrum. The area under the integrated peaks of the samples and reference concentrations of MAAs in their biological standards were used to quantify MAAs in the macroalgae (mg g^{-1} DW). Two unknown mycosporine–like amino acids were measured, one in *B. calliptera* and another in *B. montagnei*. The unknown MAA measured in *B. calliptera* exhibited maximum absorbance spectrum (λ_{max}) at 321 nm and retention time around 3.7 min, and the unknown MAA measured in *B. montagnei* exhibited λ_{max} at 330 nm and retention time around 3.9 min. These MAAs were designated as MAA 321 and MAA 330, respectively, and were quantified by applying the reference concentrations of palythine and asterina–330, respectively, based on the principle of molar extinction coefficients, palythine: e320 = 36200 (Takano et al., 1978) and asterina–330: e330 = 43500 (Gleason, 1993). Additionally, in both species one unknown mycosporine–like amino acid (designated as MAA 356) was measured by retention time (around 11.45 min) and maximum absorbance spectrum (356 nm), but could not be quantified.

Statistical analyses

The physiological responses (RGR, F_v/F_m, α, β, $rETR_{max}$, Y [II], Y[NPQ], Y[NO], pigment and MAA contents) were compared among PFD treatments for *B. calliptera* and *B. montagnei* by one–way analysis of variance (ANOVA) or Kruskal–Wallis' test when residuals did not show normality by the Shapiro–Wilk's test and homogeneity of variance by the Levene's test (Table S1). When significant differences were found by one–way ANOVA or Kruskal–Wallis' test (p< 0.05), Tukey's and Dunn's *post hoc* tests were applied, respectively. Statistical comparisons between *B. calliptera* and *B. montagnei* were made applying Student's t tests or Wilcoxon–Mann–Whitney's tests, when residuals did not show normality and homogeneity of variance. The effective quantum yield ($\Delta F/F_m'$) of both species was compared among PFD treatments, time, and species by three-way repeated measures ANOVA (Table S2).

Results

Effective quantum yield over time

In both species, effective quantum yield ($\Delta F/F_m'$) under increase in PFDs was reduced over time (Figure 1 and Table S2). The negative effect of increased PFDs was more pronounced on the $\Delta F/F_m'$ of *B. montagnei* than on the $\Delta F/F_m'$ of *B. calliptera* (Figure 1 and Table S2). Both species exhibited a similar $\Delta F/F_m'$ under the lowest PFD of 170 µmol photons m^{-2} s^{-1} over time (Figure 1).

Growth

Bostrychia calliptera increased its mean growth from 170 to 638 µmol photons m^{-2} s^{-1} (Figure 2A). Its optimum growth was

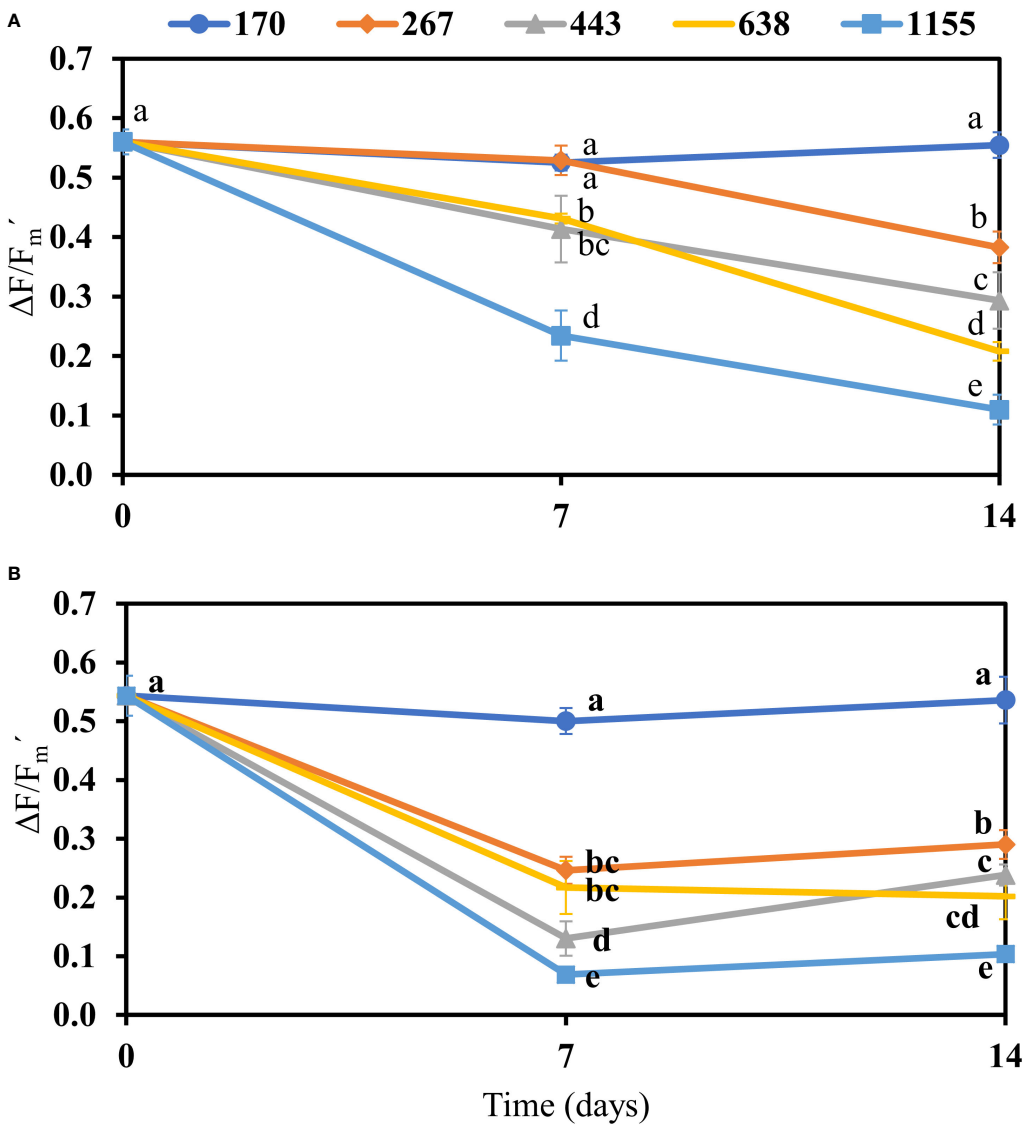

FIGURE 1
Effective quantum yield ($\Delta F/F_m'$) in photosystem II of *Bostrychia calliptera* **(A)** and *B. montagnei* **(B)** cultured under different photon flux densities (PFDs: 170, 267, 443, 638, and 1155 µmol photons m^{-2} s^{-1}) for 14 days. The effective quantum yield was measured at the beginning of experiment (time = 0) and every seven days. Symbols are means with standard deviations (bars) based on four replicates (n = 4). Different non-bold and bold letters indicate statistical differences ($p < 0.05$) among PFD treatments over time for *B. calliptera* and *B. montagnei*, respectively, by three–way repeated measures ANOVA (Table S2) and pairwise comparisons.

observed under 638 µmol photons m^{-2} s^{-1} (Figure 2A). Under 1155 µmol photons m^{-2} s^{-1} its growth was inhibited (Figure 2A). *Bostrychia montagnei* showed an optimum growth under 267 µmol photons m^{-2} s^{-1} (Figure 2B). Under PFDs from 443 to 1155 µmol photons m^{-2} s^{-1} its growth was inhibited (Figure 2B). Thus, the growth of *B. montagnei* was more negatively affected by increasing PFDs than the growth of *B. calliptera*, differing between the species (Student's t test, t = 3.05, df = 37.92, p = 0.004).

Maximum quantum yield, rETR vs. PAR curves and photosynthetic parameters

In both species a linear decrease in maximum quantum yield (F_v/F_m) was observed under increasing PFDs (Table 1). F_v/F_m did not differ between *B. calliptera* and *B. montagnei* (Wilcoxon–Mann–Whitney's test, W = 213.5, p = 0.72). Based on the relative electron transport rate (rETR) vs. photon fluence rate (PAR) curves (Figure 3), a clear pattern of

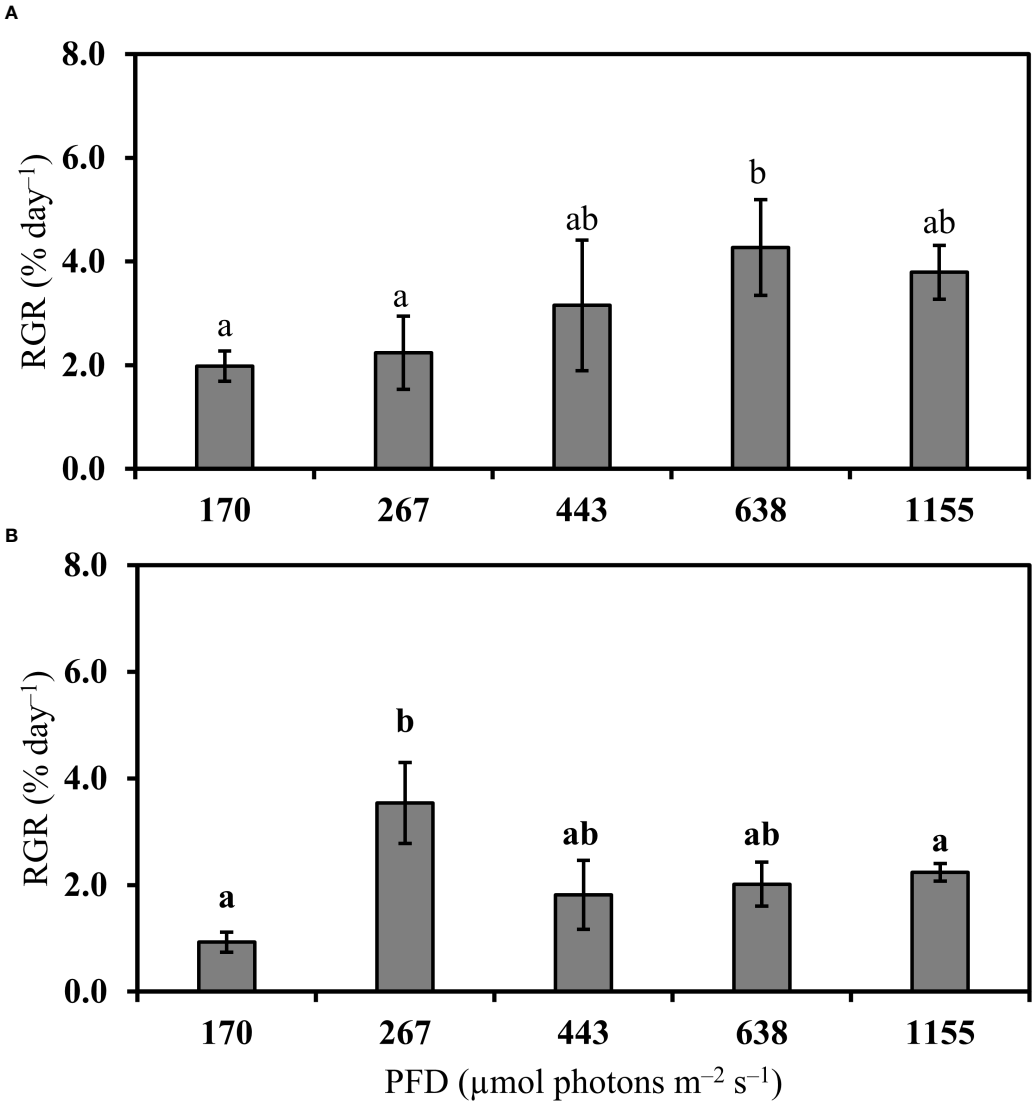

FIGURE 2
Relative growth rate (RGR, % day^{-1}) of *Bostrychia calliptera* **(A)** and *B. montagnei* **(B)** cultured under different photon flux densities (PFDs) for 14 days. Columns are means and bars are standard deviations based on four replicates (n = 4). Different non-bold and bold letters above bars indicate statistical differences (p< 0.05) among PFD treatments for *B. calliptera* and *B. montagnei*, respectively, by one–way ANOVA or Kruskal–Wallis's test (Table S1) followed by associated *post hoc* tests.

TABLE 1 Maximum quantum yield (F_v/F_m) and photosynthetic parameters of the relative electron transport rate vs. photon fluence rate curves of *Bostrychia calliptera* and *B. montagnei* cultured under different photon flux densities (PFDs in µmol photons m^{-2} s^{-1}) for 14 days.

Species	PFD	F_v/F_m	α (e photons^{-1})	β (e photons^{-1})	$rETR_{max}$ (µmol e m^{-2} s^{-1})	I_k (µmol photons m^{-2} s^{-1})
B. calliptera	170	0.581 ± 0.033^{a}	0.244 ± 0.093^{a}	-0.0021 ± 0.001^{a}	9.78 ± 0.31^{a}	46.17 ± 24.01^{a}
	267	0.429 ± 0.029^{b}	0.105 ± 0.000^{b}	-0.0024 ± 0.001^{a}	6.26 ± 1.51^{b}	59.39 ± 14.31^{a}
	443	0.321 ± 0.047^{c}	0.105 ± 0.000^{b}	-0.0023 ± 0.001^{a}	10.95 ± 3.00^{a}	103.81 ± 28.49^{b}
	638	0.203 ± 0.023^{d}	0.103 ± 0.007^{b}	-0.0083 ± 0.000^{b}	6.92 ± 1.80^{b}	67.57 ± 21.61^{ab}
	1155	0.095 ± 0.040^{e}	*	*	*	*
B. montagnei	170	0.603 ± 0.045^{A}	0.220 ± 0.031^{A}	-0.0050 ± 0.01^{A}	22.20 ± 2.45^{A}	103.17 ± 27.14^{A}
	267	0.314 ± 0.017^{B}	0.205 ± 0.100^{A}	-0.0114 ± 0.01^{B}	14.13 ± 7.81^{A}	80.37 ± 45.85^{AB}
	443	0.271 ± 0.015^{BC}	0.207 ± 0.000^{A}	-0.0119 ± 0.00^{B}	6.91 ± 0.89^{AB}	33.28 ± 4.32^{B}
	638	0.220 ± 0.034^{C}	0.107 ± 0.000^{B}	-0.0124 ± 0.00^{B}	5.43 ± 0.12^{B}	50.38 ± 1.12^{B}
	1155	0.134 ± 0.024^{D}	0.107 ± 0.000^{B}	-0.0103 ± 0.00^{B}	5.82 ± 0.00^{B}	54.00 ± 0.00^{B}

The light utilization and photoinhibition coefficients are α and β, respectively. The maximum relative electron transport rate and the saturation irradiance for photosynthesis are $rETR_{max}$ and I_k, respectively. Values are means with standard deviations based on four replicates ($n = 4$). Asterisk (*) indicates a PFD treatment for *B. calliptera* where was not possible to apply the mathematical model of Walsby (1997) due to the various zeros because of photoinhibition. Different lowercase and uppercase superscript letters indicate statistical differences ($p< 0.05$) among PFD treatments for *B. calliptera* and *B. montagnei*, respectively, by one–way ANOVA or Kruskal–Wallis' test (Table S1) followed by associated post hoc test.

decrease in rETRs of the macroalgae under light stress was only observed in *B. montagnei* (Figure 3B). This species had decreased rETRs when cultured from 170 to 1155 µmol photons m^{-2} s^{-1} (Figure 3B), pointing to photoinhibition, while *B. calliptera* only had strongly decreased rETRs when cultured at 1155 µmol photons m^{-2} s^{-1} (Figure 3A).

In relation to the photosynthetic parameters calculated from the rETR vs. PAR curves (Table 1), *B. calliptera* showed a lower light utilization coefficient (α) under PFDs of 267, 443, and 638 µmol photons m^{-2} s^{-1}, while *B. montagnei* exhibited a lower α only under 638 and 1155 µmol photons m^{-2} s^{-1} (Table 1). Overall, *B. montagnei* revealed a higher α than *B. calliptera* (0.170 ± 0.06 e photons^{-1} for *B. montagnei* and 0.111 ± 0.08 e photons^{-1} for *B. calliptera*), differing between species (Wilcoxon–Mann–Whitney's test, $W = 75$, $p< 0.001$). Regarding the photoinhibition coefficient (β), *B. calliptera* increased β only under 638 µmol photons m^{-2} s^{-1}, whereas *B. montagnei* increased β under PFD > 170 µmol photons m^{-2} s^{-1} (Table 1). Overall, *B. montagnei* showed a higher β than *B. calliptera* (-0.102 ± 0.004 e photons^{-1} for *B. montagnei* and -0.003 ± 0.002 e photons^{-1} for *B. calliptera*), differing between species (Student's t test, $t = 6.16$, df = 34.01, $p< 0.001$). A clear negative effect of increased PFDs on the maximum relative electron transport rates ($rETR_{max}$) of the macroalgae was only observed in *B. montagnei*, which decreased its $rETR_{max}$ under 638 and 1155 µmol photons m^{-2} s^{-1} (Table 1). *Bostrychia montagnei* had a lower saturation irradiance for photosynthesis (I_k) under 443, 638, and 1155 µmol photons m^{-2} s^{-1}, while the I_k of *B. calliptera* was not negatively affected by increased PFDs (Table 1). Between species, the $rETR_{max}$ and I_k did not differ significantly ($rETR_{max}$: Wilcoxon–Mann–Whitney's test, $W = 171$, $p = 0.44$; I_k: Student's t test, $t = -0.81$, df = 36.53, $p = 0.41$).

Complementary energy dissipation pathways

The use of light energy in the photochemical pathway (Y[II]) of both species decreased under increasing PFDs (Figure 4 and Table S1). The regulated non-photochemical quenching of light energy (Y[NPQ]) in both species also decreased under increasing PFDs (Figure 4 and Table S1). On the other hand, the non-regulated non-photochemical quenching of light energy (Y[NO]) increased in both species under increasing PFDs (Figure 4 and Table S1). The complementary energy dissipation pathways between *B. calliptera* and *B. montagnei* did not differ significantly (Wilcoxon–Mann–Whitney's test, Y(II): $W = 211$, $p = 0.77$; Y(NPQ): $W = 143$, $p = 0.12$; Y(NO): $W = 192.5$, $p = 0.84$).

Pigment content

The pigments phycoerythrin (PE) and allophycocyanin (APC) in *B. calliptera* did not vary significantly among PFD treatments (Figure 5A and Table S1), whereas the phycocyanin (PC) increased under 443 µmol photons m^{-2} s^{-1} in relation to 170 µmol photons m^{-2} s^{-1} (Figure 5A). Increased PFD resulted in a decrease of chlorophyll *a* (Chl *a*) in *B. calliptera* (Figure 5A and Table S1). In *B. montagnei*, the PE, PC, APC, and Chl *a* contents decreased under increased PFD (Figure 5B and Table S1). Among species, *B. calliptera* showed a higher Chl *a* content than *B. montagnei* (302.4 ± 183.4 µg g^{-1} WW in *B. calliptera* and 184.4 ± 134.7 µg g^{-1} WW in *B. montagnei*) differing statistically (Wilcoxon–Mann–Whitney's test, $W = 289$, $p = 0.01$). The PE, PC, and APC contents did not differ between species

(Wilcoxon–Mann–Whitney's test, PE: $W = 170$, $p = 0.42$; PC: $W = 259$, $p = 0.11$; APC: $W = 221$, $p = 0.58$). Only two maximum peaks of Chl absorbance were observed in the studied macroalgae, one at 664 nm and another at 410 nm, both from Chl *a* (Figures S2-3).

Mycosporine–like amino acid content

In *B. calliptera*, three mycosporine–like amino acids (MAAs) were identified and quantified: palythine, asterina–330, and porphyra–334 (Table 2). In *B. montagnei*, four MAAs were identified and quantified: palythine, asterina–330, porphyra–334, and shinorine (Table 2). In each species one unknown MAA could only be quantified, the MAA 321 in *B. calliptera* and the MAA 330 in *B. montagnei*. The main MAA in *B. calliptera* was the MAA 321, whereas in *B. montagnei* was asterina–330 (Table 2). In both species the MAA content decreased under increased PFD (Table 2). The negative effect of increased PFDs on the MAA content in *B. montagnei* was stronger than on the MAA content in *B. calliptera*, since palythine and porphyra–334 were not detected in *B. montagnei* under 443, 638, and 1155 µmol photons m^{-2} s^{-1} (Table 2). The MAA 330 was only quantified in *B. montagnei* under the lowest PFD (i.e., 170 µmol photons m^{-2} s^{-1}) (Table 2). As palythine, asterina–330,

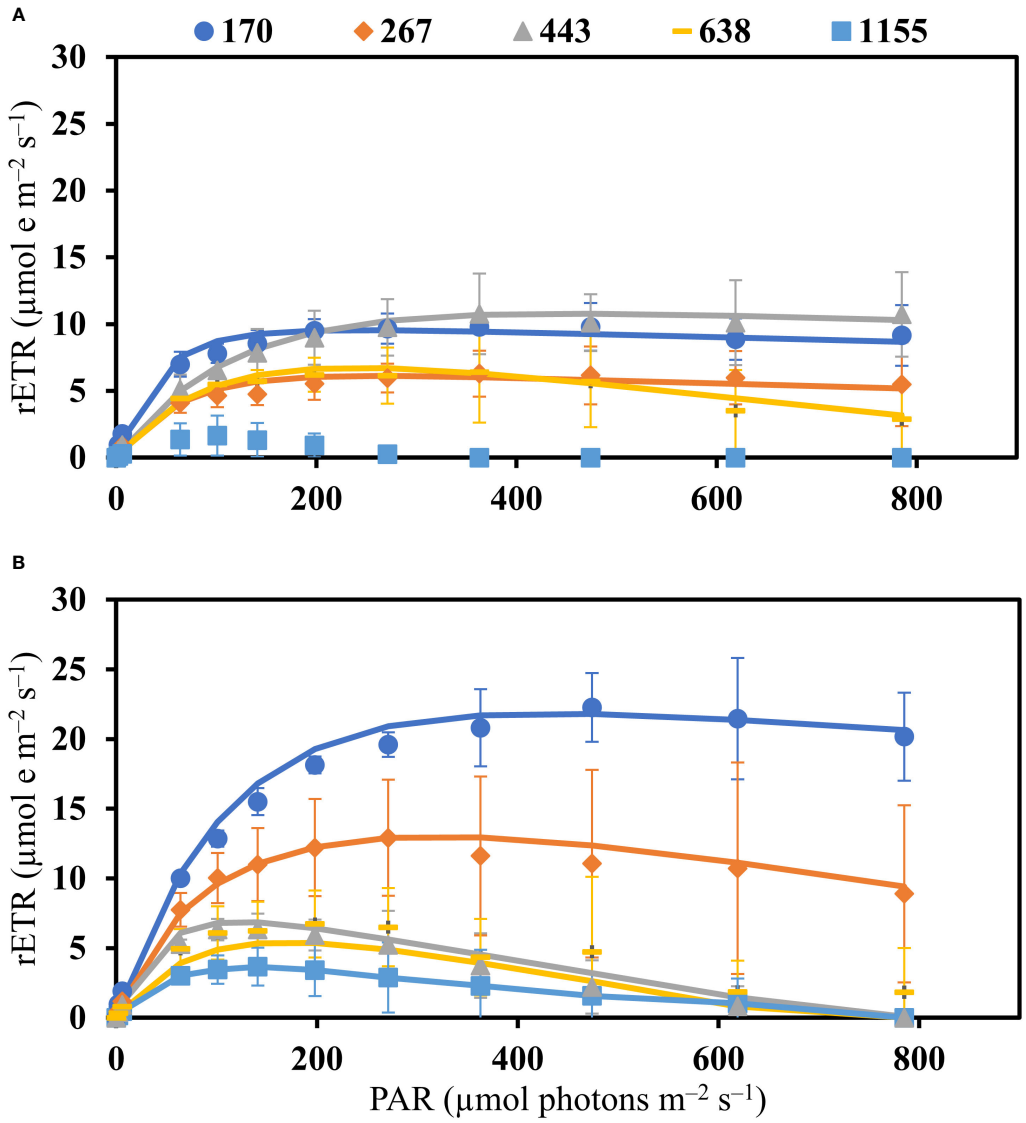

FIGURE 3
Relative electron transport rate (rETR) vs. photon fluence rate (PAR) curves of *Bostrychia calliptera* **(A)** and *B. montagnei* **(B)** cultured under different photon flux densities (PFDs: 170, 267, 443, 638, and 1155 µmol photons m^{-2} s^{-1}) for 14 days. Symbols are means with standard deviations (bars) based on four replicates ($n = 4$). Lines are rETR vs. PAR curves fitted by applying the mathematical model of Walsby (1997).

and porphyra–334 occurred simultaneously in both species, their contents were compared between *B. calliptera* and *B. montagnei*. Higher palythine and porphyra–334 contents were registered in *B. calliptera* (Table 2), differing from their contents observed in *B. montagnei* (Wilcoxon–Mann–Whitney's test, palythine: $W = 294$, $p = 0.008$; porphyra–334: $W = 332$, $p < 0.001$). The asterina–330 content did not differ between species (Wilcoxon–Mann–Whitney's test, $W = 252$, $p = 0.16$).

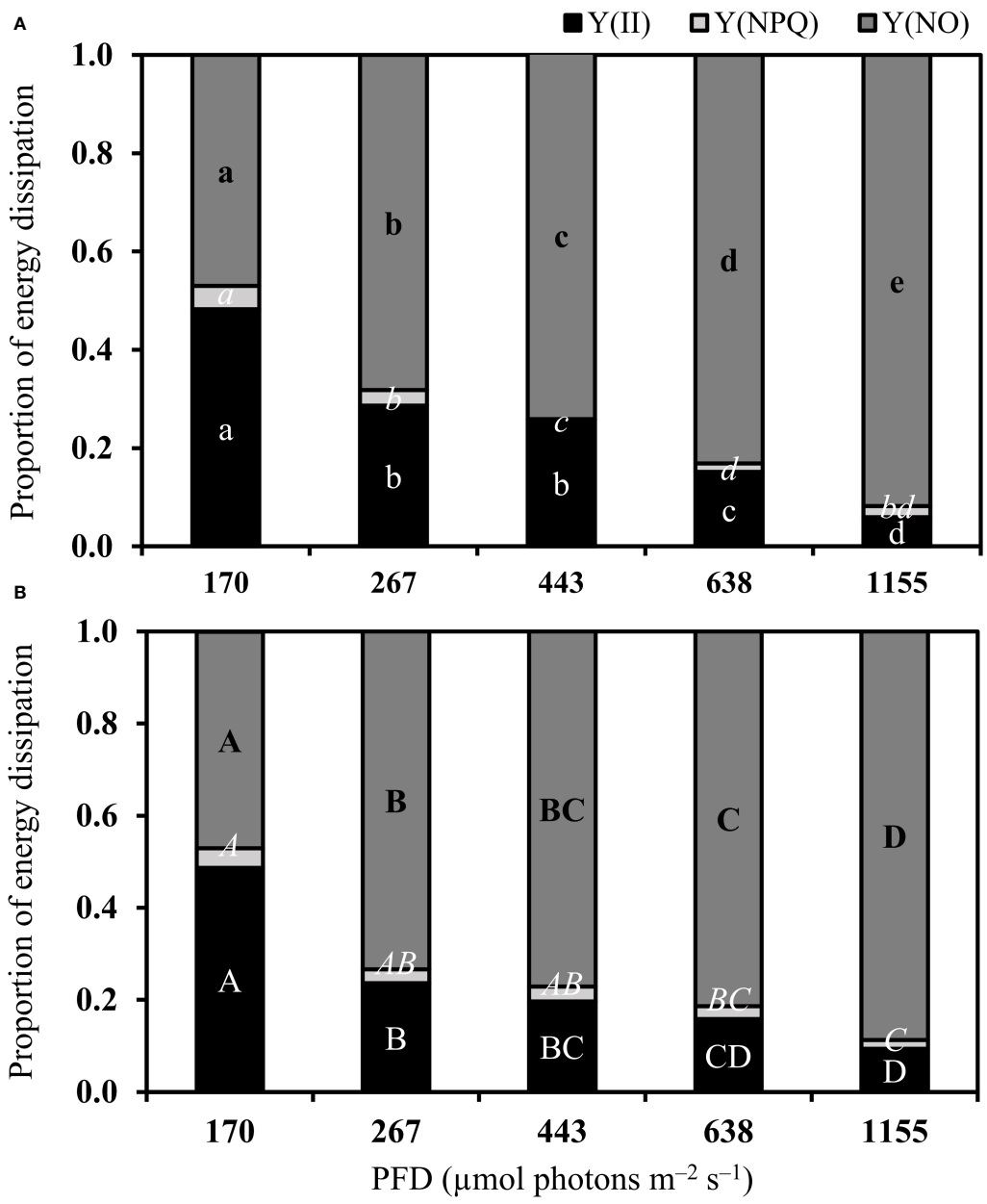

FIGURE 4
Complementary energy dissipation pathways in photosystem II of *Bostrychia calliptera* **(A)** and *B. montagnei* **(B)** cultured under different photon flux densities (PFDs) for 14 days. Columns are mean proportions of energy dissipation based on four replicates ($n = 4$). Y(II) is the photochemical pathway, Y(NPQ) is the regulated non-photochemical quenching of light energy, and Y(NO) is the non-regulated non-photochemical quenching of light energy. *Bostrychia calliptera* **(A)**: different regular, italic, and bold lowercase letters indicate statistical differences ($p < 0.05$) for Y(II), Y(NPQ), and Y(NO), respectively, among PFD treatments. *Bostrychia montagnei* **(B)**: different regular, italic, and bold uppercase letters indicate statistical differences for Y(II), Y(NPQ), and Y(NO), respectively, among PFD treatments. Statistical differences were found applying one–way ANOVA or Kruskal–Wallis' test (Table S1) followed by associated *post hoc* tests.

Discussion

Increased light conditions on estuarine ecosystems as described in the introduction will be detrimental to the physiological performance of the mangrove macroalgae *B. calliptera* and *B. montagnei*. The decline in effective and maximum quantum yield of both species under increasing PFDs (Figure 1 and Table 1) demonstrated that both macroalgae decreased the efficiency with which their PSII reaction centers captured and utilized excitation energy for photochemistry (Genty et al., 1989). This probably is related to the closed reaction centers due to high photon availability for the algal photosynthetic apparatus under increasing PFDs. Furthermore, the chlorophyll *a* content of both species was degraded under increasing light conditions (Figure 5). PSII quantum yield data are derived from chlorophyll *a* fluorescence measurements, as described in the methods section. Thus, the observed decrease in quantum yield under increasing PFD can also be explained by the reduction of chlorophyll *a* in both species. Flameling and Kromkamp

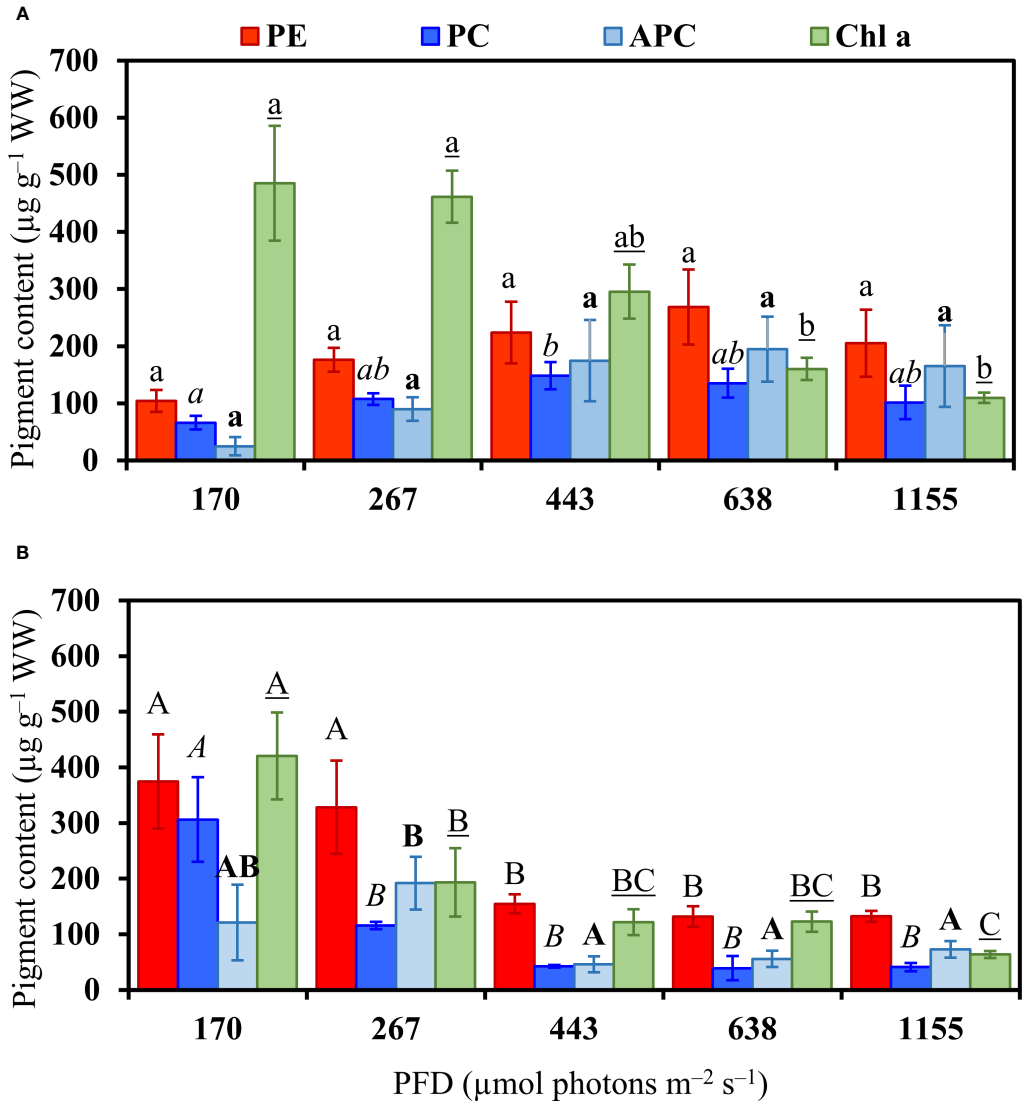

FIGURE 5
Pigment content in *Bostrychia calliptera* **(A)** and *B. montagnei* **(B)** cultured under different photon flux densities (PFDs) for 14 days. Columns are means and bars are standard deviations based on four replicates (n = 4). PE: Phycoerythrin, PC: phycocyanin, APC: allophycocyanin, Chl *a*: chlorophyll *a*. *Bostrychia calliptera* **(A)**: different regular, italic, bold, and underlined lowercase letters indicate statistical difference ($p< 0.05$) for PE, PC, APC, and Chl *a*, respectively, among PFD treatments. *Bostrychia montagnei* **(B)**: different regular, italic, bold and underlined uppercase letters indicate statistical difference for PE, PC, APC, and Chl *a*, respectively, among PFD treatments. Statistical differences were found applying one–way ANOVA or Kruskal–Wallis' test (Table S1) followed by associated *post hoc* tests.

TABLE 2 Mycosporine–like amino acid (MAA) concentrations (mg g^{-1} DW) in *Bostrychia calliptera* and *B. montagnei* cultured under different photon flux densities (PFDs in µmol photons m^{-2} s^{-1}) for 14 days.

Species	PFD	Palythine	Asterina–330	MAA 321	Porphyra–334	MAA 330	Shinorine
B. calliptera	170	0.37 ± 0.04^{a}	0.50 ± 0.08^{a}	9.16 ± 0.44^{a}	0.47 ± 010^{a}	–	–
	267	0.29 ± 0.06^{a}	0.38 ± 0.09^{ab}	6.10 ± 1.32^{b}	0.44 ± 0.12^{a}	–	–
	443	0.19 ± 0.04^{b}	0.31 ± 0.08^{b}	4.23 ± 0.76^{c}	0.36 ± 0.05^{a}	–	–
	638	0.05 ± 0.03^{c}	0.08 ± 0.05^{c}	0.83 ± 0.90^{d}	0.11 ± 0.08^{b}	–	–
	1155	–	0.04 ± 0.02^{c}	0.05 ± 0.03^{d}	0.03 ± 0.01^{b}	–	–
B. montagnei	170	$0.35 \pm 0.11^{A\star}$	2.62 ± 0.91^{A}	–	$0.66 \pm 0.12^{A\star}$	0.09 ± 0.03	0.47 ± 0.09^{A}
	267	$0.01 \pm 0.01^{B\star}$	0.11 ± 0.07^{B}	–	$0.01 \pm 0.00^{B\star}$	–	0.03 ± 0.02^{B}
	443	–	0.11 ± 0.07^{B}	–	–	–	0.05 ± 0.02^{B}
	638	–	0.09 ± 0.06^{B}	–	–	–	0.04 ± 0.01^{B}
	1155	–	0.01 ± 0.00^{B}	–	–	–	–

Values are means with standard deviations based on four replicates ($n = 4$). Dashes (–) represent PFD treatments where the MAA was not detected. Different lowercase and uppercase superscript letters indicate statistical differences ($p < 0.05$) among PFD treatments for *B. calliptera* and *B. montagnei*, respectively, by one–way ANOVA or Kruskal–Wallis' test (Table S1) followed by associated post hoc tests. Asterisks (*) indicate treatments where the statistical comparison was performed applying the Wilcoxon–Mann–Whitney test.

(1998) also reported a decrease in quantum yield of marine algae under increasing irradiances over time. The negative effect of increased PFDs on the quantum yield of *B. montagnei* was more pronounced than on the quantum yield of *B. calliptera* (Figure 1). These results are consistent with findings reported by Yokoya et al. (1999) who observed a preferential occurrence of *B. montagnei* in more shaded microhabitats in Brazilian mangroves. Our results are also consistent with Cunha and Duarte (2002) who registered a lower photosynthetic activity of *B. montagnei* (measured as photosynthetic oxygen evolution) under increasing irradiances compared to *B. calliptera*. In our study, the quantum yield of the macroalgae cultured under the lowest light stress condition (i.e., 170 µmol photons m^{-2} s^{-1}) was similar to the quantum yield of *B. scorpioides* (Hudson) Montagne subjected to lowest desiccation stress (Sánchez de Pedro et al., 2022). Thereby, quantum yield is a reliable physiological parameter to access photosynthetic performance in *Bostrychia* species. Our growth results (Figure 2) confirm the higher tolerance of *B. calliptera* to the rising light stress. This species increased its growth from 170 to 638 µmol photons m^{-2} s^{-1}, whereas *B. montagnei* reached its highest growth under 267 µmol photons m^{-2} s^{-1}. Under PFDs from 443 to 1155 µmol photons m^{-2} s^{-1} the growth of *B. montagnei* was inhibited. Light conditions affect algal growth mainly through its impact on photosynthesis. The algal growth rate is maximal at saturating irradiances for photosynthesis and decreases with both rising and declining PFDs (Kaur et al., 2022).

Based on rETR vs. PAR curves (Figure 3), a clear pattern of decline in photosynthetic performance under increasing light stress was evident for *B. montagnei*. In this species an increase in light stress was accompanied by a decrease in rETRs, whereas in *B. calliptera* the lowest rETR values were only observed under 1155 µmol photons m^{-2} s^{-1} (Figure 3). Both species exhibited a reduction in the use of light energy (α and $rETR_{max}$ as proxies) in photosynthesis and higher photoinhibition (β as a proxy) under increased light stress. Our results of saturation irradiance (I_k) for photosynthesis (Table 1) confirmed that both species are typical "shade" plants, because of the low light requirements for photosynthesis. *Bostrychia calliptera* exhibited saturation of photosynthesis under PAR values from 46.2 to 103.8 µmol photons m^{-2} s^{-1} and *B. montagnei* under PAR values from 33.3 to 103.2 µmol photons m^{-2} s^{-1}. These data are congruent with other studies performed on numerous *Bostrychia* species in which they were always characterized as typical "shade" plants (e.g., Karsten and Kirst, 1989; Karsten et al., 1993; Karsten et al., 1994a; Karsten et al., 1994b; Sánchez de Pedro et al., 2014). Our results on photosynthetic performance after culturing the macroalgae under rising light stress are consistent with findings reported by Sánchez de Pedro et al. (2014) who evaluated the photosynthetic performance of *Bostrychia scorpioides* under increasing irradiances. In their study, *B. scorpioides* also showed a decreased photosynthetic performance (measured as photosynthetic oxygen evolution) and a lower use of light energy (α as a proxy) under increased irradiance. Significant decrease in $rETR_{max}$ of *B. calliptera* under 267 µmol photons m^{-2} s^{-1} and significant increase in I_k under 443 µmol photons m^{-2} s^{-1} (Table 1) may be explained as random variation, since they did not differ from the values observed at 638 µmol photons m^{-2} s^{-1}. In our study, although *B. calliptera* was more tolerant to the increase in PFDs than *B. montagnei*, in general, higher rETRs and α were recorded in the latter species. Increased algal photosynthetic rates may be a consequence of the energy expenditures related to biochemical defenses under stress conditions (McCoy et al., 2019). Macroalgae subjected to light stress produce intracellular reactive oxygen species (ROS) (Karsten, 2008). Reactive oxygen species induce damage to macromolecular structures of the cell, including DNA, proteins, and phospholipids, which can lead to cell apoptosis

(Lesser, 2006). As a response to oxidative stress macroalgae produce several antioxidant compounds (Araújo et al., 2020; Borburema et al., 2022b). Thus, the higher photosynthetic activity recorded in *B. montagnei* (rETR and α as proxies) may be related to the energy expenditure for the biosynthesis of antioxidant defensive compounds.

Complementary energy dissipation pathway results (Figure 4) confirm the negative effect of rising light stress on both macroalgal species. The use of light energy by the photochemical pathway (Y[II]) and the regulated non–photochemical quenching of light energy (Y[NPQ]) decreased under rising PFDs, whereas the non–regulated non–photochemical quenching of light energy (Y[NO]) increased. The rise in Y(NO) at the expense of Y(II) and Y (NPQ) indicates photoinhibition or permanent damage of the photosynthetic apparatus (Klughammer and Schreiber, 2008; Graiff et al., 2021). In fact, our pigment content results (Figure 5) demonstrated that increased light conditions caused damage of the photosynthetic apparatus of *B. montagnei* and *B. calliptera*. Phycobiliprotein and chlorophyll *a* degradation was observed in *B. montagnei* under increasing light conditions, as well as chlorophyll *a* degradation was also recorded in *B. calliptera*. Sánchez de Pedro et al. (2014) also registered a decline in chlorophyll *a* content of *B. scorpioides* under increased irradiance. Pigment downregulation is a common process reported for many macroalgae under high PFDs (e.g., Figueroa et al., 1997; Celis-Plá et al., 2015), as less pigments are needed to catch enough photons to drive photosynthesis (Beer et al., 2014). Nevertheless, phycobiliproteins of *B. calliptera* were not degraded under increasing PFDs (Figure 5A). These results also support the higher tolerance observed in *B. calliptera* to increasing light stress. Chlorophyll *d* was not detected in the studied macroalgae (Figures S2-3). This could be explained as chlorophyll *d* in red algae is most likely due to a contamination of samples with cyanobacteria living in close association (Murakami et al., 2004; Hurd et al., 2014).

The MAA contents of both species decreased under rising light intensity (Table 2). This negative effect was more pronounced for *B. montagnei*, since at PFDs > 267 µmol photons m^{-2} s^{-1} the MAAs palythine and porphyra–334 could not be detected anymore and the MAA 330 was only measured at 170 µmol photons m^{-2} s^{-1} (Table 2). The assumed photodamage of the MAA contents in both *Bostrychia* species was accompanied by macroalgal bleaching (Figure S4). Nevertheless, we expected to register an increase of MAA content in both species under increasing light stress, since MAAs are photoprotective UV-sunscreen compounds (Karsten, 2008). Our results demonstrated that high PFDs have deleterious effects on the MAA concentrations of the studied macroalgae. Under low PFDs, a rise from 20 to 40 µmol photons m^{-2} s^{-1} induced *Bostrychia radicans* (Montagne) Montagne to increase its palythinol content and to synthesize other MAAs, such as myscoporine–glycine, shinorine, porphyra–334, and asterina–330 (Karsten et al., 2000). Maybe MAA biosynthesis was downregulated in macroalgae under higher PFDs to save energy for growth (Figure 2), as UVR levels did not increase with rising light intensity. Our results are consistent with Karsten et al. (1998, 2000) who also reported porphyra–334, palythine, and asterina–330 in field samples of *B. calliptera*, as well as measured these MAAs and shinorine in field samples of *B. montagnei*. In those studies, the dominant MAA in *B. calliptera* was palythine, whereas in our study was the unknown MAA designated as MAA 321 (λ_{max} at 321 nm and retention time around 3.7 min). In Karsten et al. (2000) one unknown MAA designated by those authors as MAA–1 (λ_{max} at 334 nm and retention time at 2.5 min) was dominant in *B. calliptera* as well. In our study, the dominant MAA in *B. montagnei* was asterina–330, whereas in those studies was palythinol.

In conclusion, our first hypothesis was confirmed, since increasing PFDs negatively affected the photosynthetic performance and the pigment and MAA contents of both species. Our second hypothesis was also confirmed, given that *B. calliptera* was more tolerant to the increasing light stress than *B. montagnei*. However, our third hypothesis had to be rejected, since the macroalgal MAA contents did not increase with rising light stress. The high PFDs established in our experiments decreased and eventually even degraded these UV-absorbing compounds. Overall, our results demonstrated that increased solar radiation on mangrove swamps will be harmful to the typical "shade" macroalgae *B. calliptera* and *B. montagnei*. The lower tolerance of *B. montagnei* to the increasing light stress well explains its preferential occurrence in more shaded microhabitats, as documented by Yokoya et al. (1999). Our data support that future environmental changes of increased solar radiation on coastal ecosystems will have deleterious effects on *Bostrychia* species, negatively compromising their relevant ecosystem services performed in estuarine environments.

Data availability statement

The original contributions presented in the study are included in the article/Supplementary Material. Further inquiries can be directed to the corresponding author.

Author contributions

HB, conceptualization, methodology, formal analysis, investigation, writing – original draft, and visualization. AG,

methodology, investigation, writing – review and editing. EM-S, validation, writing – review and editing. UK, validation, resources, writing – review and editing, supervision, and funding acquisition. All authors contributed to the article and approved the submitted version.

Funding

This study was financed in part by the Coordenação de Aperfeiçoamento de Pessoal de Nível Superior – Brasil (CAPES) – Finance Code 001 and 88887.586537/2020-00, Ph.D. fellowships for HB. This study was also supported by the DFG (Deutsche Forschungsgemeinschaft) under grant number GR5088/2-1.

Acknowledgments

We are grateful to Niklas Plag (University of Rostock, Applied Ecology and Phycology) for the technical support during MAA analyses by HPLC. HB is grateful to the Coordination for the Improvement of Higher Education Personnel (CAPES–Brazil) by funding his stay at University of Rostock (Germany) for research activities.

Conflict of interest

The authors declare that the research was conducted in the absence of any commercial or financial relationships that could be construed as a potential conflict of interest.

Publisher's note

Supplementary material

The Supplementary Material for this article can be found online at: https://www.frontiersin.org/articles/10.3389/fmars.2022.989454/full#supplementary-material

References

Araújo, P. G., Nardelli, A. E., Fujii, M. T., and Chow, F. (2020). Antioxidant properties of different strains of *Kappaphycus alvarezii* (rhodophyta) farmed on the Brazilian coast. *Phycologia* 59, 272–279. doi: 10.1080/00318884.2020.1736878

Beer, S., Björk, M., and Beardall, J. (2014). *Photosynthesis in the marine environment* (Wiley-Blackwell, New Jersey, USA), 224 pp.

Borburema, H. D. S., Barbosa, Ê.N.A., and Miranda, G. E. C. (2021). Decontamination protocol of the macroalga *Bostrychia binderi* Harvey (Rhodophyta) for unialgal cultures and laboratory studies. *Hoehnea* 48, e582020. doi: 10.1590/2236-8906-58/2020

Borburema, H. D. S., Lima, R. P., and Miranda, G. E. C. (2020). Effects of ocean warming, eutrophication and salinity variations on the growth of habitat-forming macroalgae in estuarine environments. *Acta Bot. Brasilica* 34, 662–672. doi: 10.1590/0102-33062020abb0303

Borburema, H. D. S., Yokoya, N. S., Soares, L. P., Souza, J. M. C., Nauer, F., Fujii, M. T., et al. (2022a). Mangrove macroalgae increase their growth under ocean acidification: A study with *Bostrychia* (rhodophyta) haplotypes from different biogeographic provinces. *J. Exp. Mar. Bio. Ecol.* 552, 151740. doi: 10.1016/j.jembe.2022.151740

Borburema, H. D. S., Yokoya, N. S., Souza, J. M. C., Nauer, F., Barbosa-Silva, M. S., and Marinho-Soriano, E. (2022b). Ocean warming and increased salinity threaten *Bostrychia* (Rhodophyta) species from genetically divergent populations. *Mar. Environ. Res.* 178, 105662. doi: 10.1016/j.marenvres.2022.105662

Celis-Plá, P. S. M., Hall-Spencer, J. M., Horta, P. A., Milazzo, M., Korbee, N., Cornwall, C. E., et al. (2015). Macroalgal responses to ocean acidification depend on nutrient and light levels. *Front. Mar. Sci.* 2. doi: 10.3389/fmars.2015.00026

Coutinho, R., and Yoneshigue, Y. (1988). Diurnal variation in photosynthesis vs. irradiance curves from "sun" and "shade" plants of *Pterocladia capillacea* (Gmelin) bornet et thuret (Gelidiaceae: Rhodophyta) from cabo frio, Rio de Janeiro, Brazil. *J. Exp. Mar. Bio. Ecol.* 118, 217–228. doi: 10.1016/0022-0981(88)90074-3

Cunha, S. R., and Costa, C. S. (2002). Gradientes de salinidade e freqüência de alagamento como determinantes da distribuição e biomassa de macroalgas associadas a troncos de manguezais Na baía de babitonga, SC. *Notas Técnicas Facimar* 6, 93–102. doi: 10.14210/bjast.v6n1.p93-102

Cunha, S. R., and Duarte, N. R. (2002). Taxas fotossintéticas e respiratórias de macroalgas do gênero *Bostrychia*. *Notas técnicas Facimar* 6, 103–110. doi: 10.14210/bjast.v6n1

Diehl, N., Michalik, D., Zuccarello, G. C., and Karsten, U. (2019). Stress metabolite pattern in the eulittoral red alga *Pyropia plicata* (Bangiales) in new Zealand – mycosporine-like amino acids and heterosides. *J. Exp. Mar. Bio. Ecol.* 510, 23–30. doi: 10.1016/j.jembe.2018.10.002

Figueroa, F. L., Celis-Plá, P. S. M., Martínez, B., Korbee, N., Trilla, A., and Arenas, F. (2019). Yield losses and electron transport rate as indicators of thermal stress in *Fucus serratus* (Ochrophyta). *Algal Res.* 41, 101560. doi: 10.1016/j.algal.2019.101560

Figueroa, F. L., Domínguez-González, B., and Korbee, N. (2014). Vulnerability and acclimation to increased UVB radiation in three intertidal macroalgae of different morpho-functional groups. *Mar. Environ. Res.* 97, 30–38. doi: 10.1016/j.marenvres.2014.01.009

Figueroa, F. L., Salles, S., Aguilera, J., Jiménez, C., Mercado, J., Viñegla, B., et al. (1997). Effects of solar radiation on photoinhibition and pigmentation in the red alga *Porphyra leucosticta*. *Mar. Ecol. Prog. Ser.* 151, 81–90. doi: 10.3354/meps151081

Flameling, I. A., and Kromkamp, J. (1998). Light dependence of quantum yields for PSII charge separation and oxygen evolution in eucaryotic algae. *Limnol. Oceanogr.* 43, 284–297. doi: 10.4319/lo.1998.43.2.0284

Fontes, K. A. A., Pereira, S. M. B., and Zickel, C. S. (2007). Macroalgas do "Bostrychietum" aderido em pneumatóforos de duas áreas de manguezal do estado de pernambuco, brasil. *Iheringia - Ser. Bot.* 62, 31–38. https://isb.emnuvens.com.br/iheringia/article/view/170

Gambichler, V., Zuccarello, G. C., and Karsten, U. (2021a). Physiological responses to salt stress by native and introduced red algae in new Zealand. *Algae* 36, 137–146. doi: 10.4490/algae.2021.36.6.10

Gambichler, V., Zuccarello, G. C., and Karsten, U. (2021b). Seasonal changes in stress metabolites of native and introduced red algae in new Zealand. *J. Appl. Phycol.* 33, 1157–1170. doi: 10.1007/s10811-020-02365-0

García, A. F., Bueno, M., and Leite, F. P. P. (2016). The bostrychietum community of pneumatophores in araçá bay: An analysis of the diversity of macrofauna. *J. Mar. Biol. Assoc. United Kingdom* 96, 1617–1624. doi: 10.1017/S0025315415001964

Genty, B., Briantais, J. M., and Baker, N. R. (1989). The relationship between the quantum yield of photosynthetic electron transport and quenching of chlorophyll fluorescence. *Biochim. Biophys. Acta* 990, 87–92. doi: 10.1016/S0304-4165(89)80016-9

Gleason, D. F. (1993). Differential effects of ultraviolet radiation on green and brown morphsof the carribean coral *Porites astreoides*. *Limnol. Oceangr.* 38, 1452–1463. doi: 10.4319/lo.1993.38.7.1452

Graiff, A., Bartsch, I., Glaser, K., and Karsten, U. (2021). Seasonal photophysiological performance of adult Western Baltic *Fucus vesiculosus* (Phaeophyceae) under ocean warming and acidification. *Front. Mar. Sci.* 8. doi: 10.3389/fmars.2021.666493

Hurd, C. L., Harrison, P. J., Bischof, K., and Lobban, C. S. (2014). *Seaweed ecology and physiology. 2nd ed* (Cambridge University Press: Cambridge, UK). doi: 10.1017/CBO9781139192637

INPE (2022) *Instituto nacional de pesquisas espaciais. divisão de satèlites e sistemas ambientais*. Available at: http://satelite.cptec.inpe.br/radiacao/.

IPCC (2014). *Climate change 2014: Synthesis report. contribution of working groups I, II and III to the fifth assessment report of the intergovernmental panel on climate change*. Eds. K. P. R., A. M. L., et al (Switzerland: IPCC). doi: 10.1017/CBO9781107415324.004

IPCC (2019). ""Summary for policymakers,"," in *IPCC special report on the ocean and cryosphere in a changing climate*. Eds. H.-O. Pörtner, D. C. Roberts, V. Masson-Delmotte, P. Zhai, M. Tignor, E. Poloczanska, et al, 34, 1843–1869. Available at: http://www.ipcc.ch/publications_and_data/ar4/wg2/en/spm.html. (Switzerland: IPCC)

Jeffrey, S. W., and Humphrey, G. F. (1975). New spectrophotometric equations for determining chlorophylls a, b, c1 and c2 in higher plants, algae and natural phytoplankton. *Biochem. und Physiol. der Pflanz.* 167, 191–194. doi: 10.1016/s0015-3796(17)30778-3

Karsten, U. (2008). "Defense strategies of algae and cyanobacteria against solar ultraviolet radiation," in *Algal chemical ecology*. Ed. C. D. Amsler (Berlin: Springer-Verlag), 273–296. doi: 10.1007/978-3-540-74181-7_13

Karsten, U., and Kirst, G. O. (1989). The effect of salinity on growth, photosynthesis and respiration in the estuarine red alga *Bostrychia radicans*. *Helgolander Meresunters* 43, 61–66. doi: 10.1007/BF02365550

Karsten, U., Koch, S., Kirst, G. O., and West, J. A. (1996). Physiological responses of the eulittoral macroalga *Stictosiphonia hookeri* (Rhodomelaceae, rhodophyta) from Argentina and Chile: Salinity, light and temperature acclimation. *Eur. J. Phycol.* 31, 361–368. doi: 10.1080/09670269600651591

Karsten, U., Koch, S., West, J. A., and Kirst, G. O. (1994a). The intertidal red alga *Bostrychia simpliciuscula* Harvey ex j. agardh from a mangrove swamp in Singapore: acclimation to light and salinity. *Aquat. Bot.* 48, 313–323. doi: 10.1016/0304-3770(94)90023-X

Karsten, U., Sawall, T., West, J., and Wiencke, C. (2000). Ultraviolet sunscreen compounds in epiphytic red algae from mangroves. *Hydrobiologia* 1, 159–171. doi: 10.1023/A:1004046909810

Karsten, U., Sawall, T., and Wiencke, C. (1998). A survey of the distribution of UV-absorbing substances in tropical macroalgae. *Phycol. Res.* 46, 271–279. doi: 10.1046/j.1440-1835.1998.00144.x

Karsten, U., West, J. A., and Ganesan, E. K. (1993). Comparative physiological ecology of *Bostrychia moritziana* (Ceramiales, rhodophyta) from freshwater and marine habitats. *Phycologia* 32, 401–409. doi: 10.2216/i0031-8884-32-6-401.1

Karsten, U., West, J. A., Zuccarello, G. C., and Kirst, G. O. (1994b). Physiological ecotypes in the marine alga *Bostrychia radicans* (Ceramiales, rhodophyta) from the east coast of the U.S.A. *J. Phycol.* 30, 174–182. doi: 10.1111/j.0022-3646.1994.00174.x

Kaur, M., Saini, K. C., Ojah, H., Sahoo, R., Gupta, K., Kumar, A., et al. (2022). Abiotic stress in algae: response, signaling and transgenic approaches. *J. Appl. Phycol.* 34, 1843–1869. doi: 10.1007/s10811-022-02746-7

Kieckbusch, D. K., Koch, M. S., Serafy, J. E., and Anderson, W. T. (2004). Trophic linkages among primary producers and consumers in fringing mangroves of subtropical lagoons. *Bull. Mar. Sci.* 74, 271–285. https://www.ingentaconnect.com/contentone/umrsmas/bullmar/2004/00000074/00000002/art00003

King, R. J., and Puttock, C. F. (1989). The morphology and taxonomy of *Bostrychia* montagne and *Stictosiphonia* j. hooker et Harvey (Rhodomelaceae, rhodophyta). *Aust. Syst. Bot.* 3, 1–73. doi: 10.1071/SB9890001

Klughammer, C., and Schreiber, U. (2008). Complementary PS II quantum yields calculated from simple fluorescence parameters measured by PAM fluorometry and the saturation pulse method. *PAM Appl. Notes* 1, 27–35. https://www.walz.com/files/downloads/pan/PAN078007.pdf

Kursar, T. A., van der Meer, J., and Alberte, R. S. (1983). Light-harvesting system of the red alga *Gracilaria tikvahiae*. *Plant Physiol.* 73, 353–360. doi: 10.1104/pp.73.2.353

Lalegerie, F., Lajili, S., Bedoux, G., Taupin, L., Stiger-Pouvreau, V., and Connan, S. (2019). Photo-protective compounds in red macroalgae from Brittany: Considerable diversity in mycosporine-like amino acids (MAAs). *Mar. Environ. Res.* 147, 37–48. doi: 10.1016/j.marenvres.2019.04.001

Lesser, M. P. (2006). Oxidative stress in marine environments: Biochemistry and physiological ecology. *Annu. Rev. Physiol.* 68, 253–278. doi: 10.1146/annurev.physiol.68.040104.110001

Machado, G. E. M., and Nassar, C. A. G. (2007). Assembléia de macroalgas de dois manguezais do núcleo picinguaba - parque estadual da serra do mar, são paulo, brasil. *Rodriguésia* 58, 835–846. doi: 10.1590/2175-7860200758408

Machado, G. E. M., Nassar, C. A. G., and de Széchy, M. T. M. (2011). Phycological flora from the shallow sublittoral zone of the rocky shores of serra do mar state park, ubatuba, são paulo. *Acta Bot. Brasilica* 25, 71–82. doi: 10.1590/S0102-33062011000100010

Madronich, S. (1992). Implications of recent total atmospheric ozone measurements for biological active ultraviolet radiation reaching the earth's surface. *Geophys. Res. Lett.* 19, 37–40. doi: 10.1029/91GL02954

McCoy, S. J., Santillán-Sarmiento, A., Brown, M. T., Widdicombe, S., and Wheeler, G. L. (2019). Photosynthetic responses of turf-forming red macroalgae to high CO_2 conditions. *J. Phycol.* 56, 85–96. doi: 10.1111/jpy.12922

Melville, F., and Pulkownik, A. (2006). Investigation of mangrove macroalgae as bioindicators of estuarine contamination. *Mar. pollut. Bull.* 52, 1260–1269. doi: 10.1016/j.marpolbul.2006.02.021

Melville, F., and Pulkownik, A. (2007). Investigation of mangrove macroalgae as biomonitors of estuarine metal contamination. *Sci. Total Environ.* 387, 301–309. doi: 10.1016/j.scitotenv.2007.06.036

Mendonça, I. R. W., and da Cunha Lana, P. (2021). Richness and biomass distribution of the mangrove macroalgal association in a subtropical estuary. *Ocean Coast. Res.* 69, e21032. doi: 10.1590/2675-2824069.21006irwm

Murakami, A., Miyashita, H., Iseki, M., Adachi, K., and Mimuro, M. (2004). Chlorophyll d in an epiphytic cyanobacterium of red algae. *Science* 303, 5664. doi: 10.1126/science.1095459

Orfanoudaki, M., Hartmann, A., Miladinovic, H., Ngoc, H. N., Karsten, U., and Ganzera, M. (2019). Bostrychines a–f, six novel mycosporine-like amino-acids and a novel betaine from the red alga *Bostrychia scorpioides*. *Mar. Drugs* 17, 356. doi: 10.3390/md17060356

Orfanoudaki, M., Hartmann, A., Ngoc, H. N., Gelbrich, T., West, J., Karsten, U., et al. (2020). Mycosporine-like amino acids, brominated and sulphated phenols: Suitable chemotaxonomic markers for the reassessment of classification of *Bostrychia calliptera* (Ceramiales, rhodophyta). *Phytochemistry* 174, 112344. doi: 10.1016/j.phytochem.2020.112344

Pedroche, F. F., West, J. A., Zuccarello, G. C., and Karsten, U. (1995). Marine red algae of the mangroves in pacific Mexico and Guatemala. *Bot. Mar.* 38, 111–119. doi: 10.1515/botm.1992.35.6.567

Post, E. (1936). Systematische und pflanzengeographische notizen zur *Bostrychia-Caloglossa* assoziation. *Rev. Algol.* 9, 1–84. https://www.biodiversitylibrary.org/item/281366#page/1/mode/1up

Raven, J. A., Smith, F. A., and Glidewell, S. M. (1979). Photosynthetic capacities and biological strategies of giant-celled and small-celled macroalgae. *New Phytol.* 83, 299–309. doi: 10.1111/j.1469-8137.1979.tb07455.x

Rios-Marin, F., Peña-Salamanca, E. J., and Benítez-Benítez, R. (2021). Efecto del pH en las tasas de bioacumulación de metales pesados en la macroalga *Bostrychia calliptera* (Rhodomelaceae, ceramiales). *Acta Biológica Colomb.* 26, 226–234. doi: 10.15446/abc.v26n2.84142

Sánchez de Pedro, R., Niell, F. X., and Carmona, R. (2014). Understanding the intertidal zonation of two macroalgae from ex situ photoacclimation responses. *Eur. J. Phycol.* 49, 538–549. doi: 10.1080/09670262.2014.978394

Sánchez de Pedro, R., Niell, F. X., and Carmona, R. (2022). Close but distant: Emersion promotes ecophysiological differentiation between two rhodophytes within an estuarine intertidal zone. *J. Exp. Mar. Bio. Ecol.* 547, 151664. doi: 10.1016/j.jembe.2021.151664

Sassi, R., Kutner, M. B. B., and Moura, G. F. (1988). Studies on the decomposition of drift seaweed from the northeast Brazilian coastal reefs. *Hydrobiologia* 157, 187–192. doi: 10.1007/BF00006971

Scherner, F., Ventura, R., Barufi, J. B., and Horta, P. A. (2013). Salinity critical threshold values for photosynthesis of two cosmopolitan seaweed species: Providing baselines for potential shifts on seaweed assemblages. *Mar. Environ. Res.* 91, 14–25. doi: 10.1016/j.marenvres.2012.05.007

Scherrer, K. J. N., Kortsch, S., Varpe, O., Weyhenmeyer, G. A., Gulliksen, B., and Primicerio, R. (2019). Mechanistic model identifies increasing light availability due to sea ice reductions as cause for increasing macroalgae cover in the Arctic. *Limnol. Oceanogr.* 64, 330–341. doi: 10.1002/lno.11043

Schmidt, É.C., Pereira, B., dos Santos, R. W., Gouveia, C., Costa, G. B., Faria, G. S. M., et al. (2012). Responses of the macroalgae *Hypnea musciformis* after *in vitro* exposure to UV-b. *Aquat. Bot.* 100, 8–17. doi: 10.1016/j.aquabot.2012.03.004

Schreiber, U., Bilger, W., and Neubauer, C. (1995). Chlorophyll fluorescence as a nonintrusive indicator for rapid assessment of *In vivo* photosynthesis. In: *Ecophysiol. Photosynth.*, Eds. E.-D. Schulze and M. M. Caldwell Springer-Verlag: Berlin Heidelberg. 49–70. doi: 10.1007/978-3-642-79354-7_3

Souza, J. M. C., and Yokoya, N. S. (2016). Effects of cytokinins on physiological and biochemical responses of the agar-producing red alga *Gracilaria caudata* (Gracilariales, rhodophyta). *J. Appl. Phycol.* 28, 3491–3499. doi: 10.1007/s10811-016-0885-5

Starr, R., and Zeikus, J. (1993). UTEX-the culture collection of algae at the university of Texas at Austin 1993 list of cultures. *J. Phycol.* 23(Suppl 2), 1–106. doi: 10.1111/j.0022-3646.1993.00001.x

Suggett, D. J., Prášil, O., and Borowitzka, M. A. (2011). *Chlorophyll a fluorescence in aquatic sciences* (Dordrecht Heidelberg London New York). doi: 10.1007/978-90-481-9268-7

Takano, S., Uemura, D., and Hirata, Y. (1978). Isolation and structure of a new amino acid, palythine, from the zoanthid *Palythoa tuberculosa*. *Tetrahedron Lett.* 26, 2299–2300. doi: 10.1016/S0040-4039(01)91519-9

Thomas, P., Swaminathan, A., and Lucas, R. M. (2012). Climate change and health with an emphasis on interactions with ultraviolet radiation: a review. *Glob. Change Biol.* 18, 2392–2405. doi: 10.1111/j.1365-2486.2012.02706.x

Valiela, I. (1984). *Marine ecological processes* (New York: Springer-Verlag), 686 pp.

Van de Poll, W. H., Eggert, A., Buma, A. G. J., and Breeman, A. M. (2001). Effects of UV-b-induced DNA damage and photoinhibition on growth of temperate marine red macrophytes: Habitat-related differences in UV-b tolerance. *J. Phycol.* 37, 30–38. doi: 10.1046/j.1529-8817.2001.037001030.x

Vieira, E. A., Filgueiras, H. R., Bueno, M., Leite, F. P. P., and Dias, G. M. (2018). Co-Occurring morphologically distinct algae support a diverse associated fauna in the intertidal zone of araçá bay, Brazil. *Biota Neotrop.* 18, 1–8. doi: 10.1590/1676-0611-bn-2017-0464

Walsby, A. E. (1997). Numerical integration of phytoplankton photosynthesis through time and depth in a water column. *New Phytol.* 136, 189–209. doi: 10.1046/j.1469-8137.1997.00736.x

West, J. A., Zuccarello, G. C., Pedroche, F. F., and Karsten, U. (1992). Marine red algae of the mangroves in pacific Mexico and their polyol content. *Bot. Mar.* 35, 567–572. doi: 10.1515/botm.1992.35.6.567

Yokoya, N. S., Plastino, E. M., Braga, M. R. A., Fujii, M. T., Cordeiro-Marino, M., Eston, V. R., et al. (1999). Temporal and spatial variations in the structure of macroalgal communities associated with mangrove trees of ilha do cardoso, são paulo state, Brazil. *Rev. Bras. Botânica* 22, 195–204. doi: 10.1590/s0100-84041999000200010

Yong, Y. S., Yong, W. T. L., and Anton, A. (2013). Analysis of formulae for determination of seaweed growth rate. *J. Appl. Phycol.* 25, 1831–1834. doi: 10.1007/s10811-013-0022-7